

## LETTERS

# BRAF<sup>E600</sup>-associated senescence-like cell cycle arrest of human naevi

Chrysiis Michaloglou<sup>1\*</sup>, Liesbeth C. W. Vredeveld<sup>1\*</sup>, Maria S. Soengas<sup>3\*</sup>, Christophe Denoyelle<sup>3</sup>, Thomas Kuilman<sup>1</sup>, Chantal M. A. M. van der Horst<sup>4</sup>, Donné M. Majoor<sup>2</sup>, Jerry W. Shay<sup>5</sup>, Wolter J. Mooi<sup>6</sup> & Daniel S. Peeper<sup>1</sup>

Most normal mammalian cells have a finite lifespan<sup>1</sup>, thought to constitute a protective mechanism against unlimited proliferation<sup>2–4</sup>. This phenomenon, called senescence, is driven by telomere attrition, which triggers the induction of tumour suppressors including p16<sup>INK4a</sup> (ref. 5). In cultured cells, senescence can be elicited prematurely by oncogenes<sup>6</sup>; however, whether such oncogene-induced senescence represents a physiological process has long been debated. Human naevi (moles) are benign tumours of melanocytes that frequently harbour oncogenic mutations (predominantly V600E, where valine is substituted for glutamic acid) in BRAF<sup>7</sup>, a protein kinase and downstream effector of Ras. Nonetheless, naevi typically remain in a growth-arrested state for decades and only rarely progress into malignancy (melanoma)<sup>8–10</sup>. This raises the question of whether naevi undergo BRAF<sup>V600E</sup>-induced senescence. Here we show that sustained BRAF<sup>V600E</sup> expression in human melanocytes induces cell cycle arrest, which is accompanied by the induction of both p16<sup>INK4a</sup> and senescence-associated acidic  $\beta$ -galactosidase (SA- $\beta$ -Gal) activity, a commonly used senescence marker. Validating these results *in vivo*, congenital naevi are invariably positive for SA- $\beta$ -Gal, demonstrating the presence of this classical senescence-associated marker in a largely growth-arrested, neoplastic human lesion. In growth-arrested melanocytes, both *in vitro* and *in situ*, we observed a marked mosaic induction of p16<sup>INK4a</sup>, suggesting that factors other than p16<sup>INK4a</sup> contribute to protection against BRAF<sup>V600E</sup>-driven proliferation. Naevi do not appear to suffer from telomere attrition, arguing in favour of an active oncogene-driven senescence process, rather than a loss of replicative potential. Thus, both *in vitro* and *in vivo*, BRAF<sup>V600E</sup>-expressing melanocytes display classical hallmarks of senescence, suggesting that oncogene-induced senescence represents a genuine protective physiological process.

Melanocytic naevi represent an intriguing human setting where an activated oncogene can co-exist with long-term arrested cells. Naevi are very common, clonal and benign tumours of cutaneous melanocytes<sup>11</sup>, and frequently harbour the V600E mutation in BRAF<sup>7</sup> (NCBI gene bank re-named the V599E mutation based on newly available sequence data; accession number NM\_004333.2; hereafter referred to as BRAF<sup>E600</sup>). However, in spite of the oncogenic nature of this mutation<sup>12,13</sup>, an initial phase of naevus growth is typically followed by a near-complete cessation of proliferative activity, which is maintained for many decades<sup>8,9,14</sup>. Therefore, it is conceivable that growth arrest of naevi results from oncogene-induced

senescence acting as an effective cellular brake against BRAF<sup>E600</sup>-mediated oncogenic signalling.

To test this hypothesis, we first determined the effect of the naevus-associated BRAF<sup>E600</sup> mutant on the proliferative capacity of freshly isolated normal human skin melanocytes. A bicistronic lentiviral vector co-expressing BRAF<sup>E600</sup> and enhanced green fluorescent protein (eGFP) (to monitor infection efficiency, typically approximately 90%; Fig. 1a) was used to transduce melanocytes. Short-term expression of BRAF<sup>E600</sup> (3–7 days) led to enhanced melanocyte proliferation that was measured by a moderate but reproducible increase in 5-bromodeoxyuridine (BrdU) incorporation (Fig. 1b and data not shown). However, this effect was transient—sustained expression of BRAF<sup>E600</sup> resulted in marked cell cycle arrest. In most (roughly 80%) of the transduced melanocytes, this was associated with an intense activity of SA- $\beta$ -Gal, a marker for senescent or stressed cultured cells as well as for aged tissues *in vivo*<sup>6,15</sup> (Fig. 1c).

The p16<sup>INK4a</sup> protein is a major tumour suppressor, often highly expressed in senescent cells *in vitro* and inactivated in a variety of human cancers, including 30–70% of melanomas<sup>16</sup>. We found that BRAF<sup>E600</sup>-expressing melanocytes had elevated levels of p16<sup>INK4a</sup> (Fig. 1d). Notably, the staining for p16<sup>INK4a</sup> was heterogeneous, with 25–35% of the BRAF<sup>E600</sup>-expressing melanocytes showing low or undetectable p16<sup>INK4a</sup> levels, in spite of the fact that over 95% of these cells were arrested (and still expressed the lentiviral cassette, as evident from eGFP expression).

As oncogene-induced senescence *in vitro* has been best defined in primary diploid fibroblasts, we analysed the cellular response to activated BRAF in this 'reference' context. Consistent with previous results obtained with overexpression of Ras<sup>V12</sup> or Raf1 (refs 6, 17, 18), retroviral delivery of BRAF<sup>E600</sup> into two different strains of normal human fibroblasts caused a complete cessation of proliferation, along with induction of p16<sup>INK4a</sup> (see Supplementary Fig. 1a, b). To exclude the possibility that these effects were caused by supra-physiological levels of BRAF<sup>E600</sup> expression, we designed a system in which its expression levels could be manipulated with considerable precision. Cells were transduced with a mixture of retrovirus encoding a BRAF<sup>E600</sup> expression cassette and retrovirus encoding a short hairpin (sh)RNA targeting both endogenous wild type and ectopic BRAF<sup>E600</sup> (for details, see Fig. 2 legend). This strategy allowed expression of BRAF<sup>E600</sup> to levels similar to those seen in melanoma cells (see Supplementary Fig. 2a), or to levels close to, or indistinguishable from, endogenous BRAF levels (Fig. 2a, compare lanes 4 and 5).

<sup>1</sup>Division of Molecular Genetics and <sup>2</sup>Division of Pathology, The Netherlands Cancer Institute, Plesmanlaan 121, 1066 CX Amsterdam, The Netherlands. <sup>3</sup>Department of Dermatology and Comprehensive Cancer Center, University of Michigan, 1500 E Medical Center Dr. Ann Arbor, Michigan 48109, USA. <sup>4</sup>Department of Plastic, Reconstructive and Hand Surgery, Academic Medical Centre, PO Box 22660 G4-226, 1100 AZ Amsterdam, The Netherlands. <sup>5</sup>Department of Cell Biology and Harold Simmons Cancer Center, The University of Texas Southwestern Medical Center, 5323 Harry Hines Boulevard, Dallas, Texas 75390, USA. <sup>6</sup>Department of Pathology, Free University Medical Centre, De Boelelaan 1117, 1081 HV Amsterdam, The Netherlands.

\*These authors contributed equally to this work.

The elevation of p16<sup>INK4a</sup> levels was maintained on progressively diminishing BRAF<sup>E600</sup> levels (see Supplementary Fig. 2a). We did not see upregulation of p14<sup>ARF</sup> by BRAF<sup>E600</sup> (see Supplementary Fig. 3). Furthermore, low levels of BRAF<sup>E600</sup> caused inhibition of both DNA replication (see Supplementary Fig. 2b) and cellular proliferation (Fig. 2b). This arrest was stably maintained, without any significant escape (see Supplementary Fig. 2c). However, it was bypassed by co-expression of the SV40 large tumour antigen (see Supplementary Fig. 2d), arguing against an aphysiological effect and suggesting that

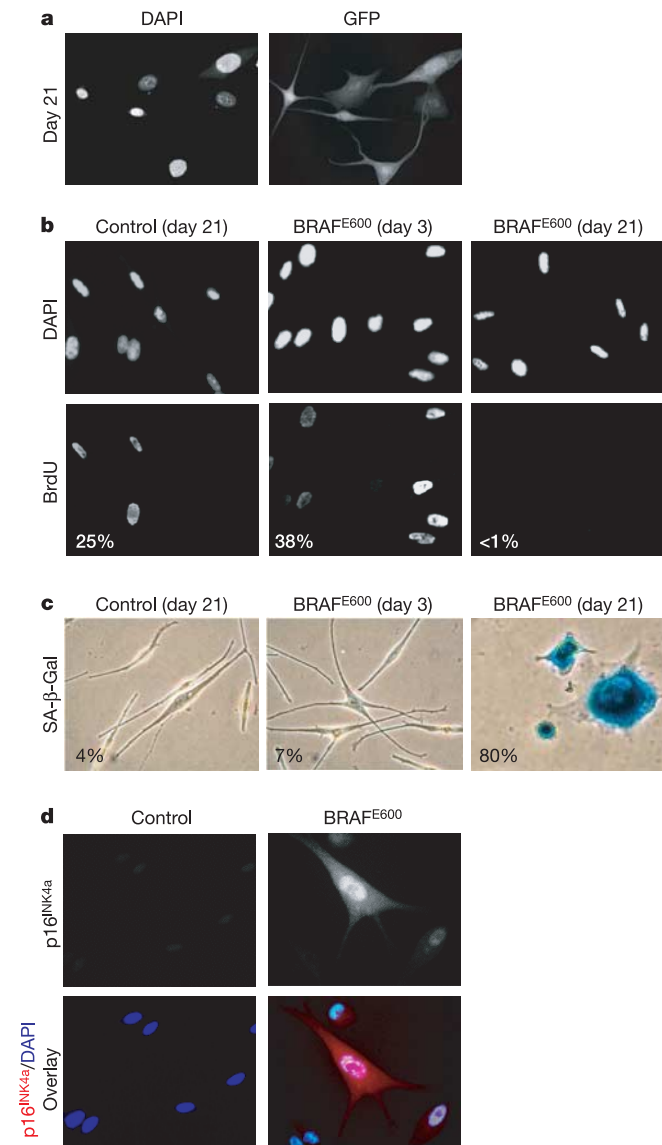


**Figure 1 | Sustained expression of BRAF<sup>E600</sup> induces a senescence-like arrest in normal human melanocytes.** **a**, Infection efficiency is estimated to be approximately 90% by visualization of eGFP-positive cells. Nuclear staining by DAPI is shown as an indication of total cell number. **b**, Impact of BRAF<sup>E600</sup> on melanocyte proliferation measured as the percentage of positive cells after a 3-h pulse with BrdU. DAPI stain to detect nuclei (top panel) and BrdU-positive cells (bottom panel). Control melanocytes remained proliferative and viable. **c**, SA-β-Gal activity after brief and sustained BRAF<sup>E600</sup> expression. **d**, Heterogeneous levels of p16<sup>INK4a</sup> (upper panels and lower panels, red) in BRAF<sup>E600</sup>-transduced melanocytes. DAPI stain is used to detect nuclei (lower panels, blue). Note that at 21 days after infection, <1% of the BRAF<sup>E600</sup>-expressing melanocytes incorporated BrdU, the vast majority showed positive SA-β-Gal activity, whereas a smaller proportion of BRAF<sup>E600</sup>-expressing cells had detectable p16<sup>INK4a</sup> expression. Numbers given are representative of three independent experiments.

this arrest depends on cellular tumour suppressors. Furthermore, in the context of fibroblasts defective for p53 and p16<sup>INK4a</sup> and expressing SV40 small tumour antigen and human telomerase reverse transcriptase (hTERT), BRAF<sup>E600</sup> could efficiently substitute for Ras<sup>V12</sup> in the induction of tumours in immunocompromised mice (see Supplementary Table 1).

Recently, overexpression of Ras<sup>V12</sup> has been shown to cause accumulation of senescence-associated heterochromatic foci (SAHF), concentrated spots of transcriptionally silenced DNA<sup>19</sup>. We observed that low levels of BRAF<sup>E600</sup> also induced SAHF (Fig. 2c). This was accompanied by focal accumulation of a specific heterochromatin-associated histone modification, namely methylation of lysine 9 of histone H3 (K9M-H3). Together, these results indicate that low levels of BRAF<sup>E600</sup> induce senescence-like cell cycle arrest in primary human cells.

To investigate whether p16<sup>INK4a</sup> upregulation constitutes a protective response to inappropriate mitogenic signalling by BRAF<sup>E600</sup>, we created cell lines stably expressing p16<sup>INK4a</sup> shRNA. This shRNA was effective, as it suppressed the accumulation of p16<sup>INK4a</sup> in various settings (Fig. 2a), caused increased proliferation

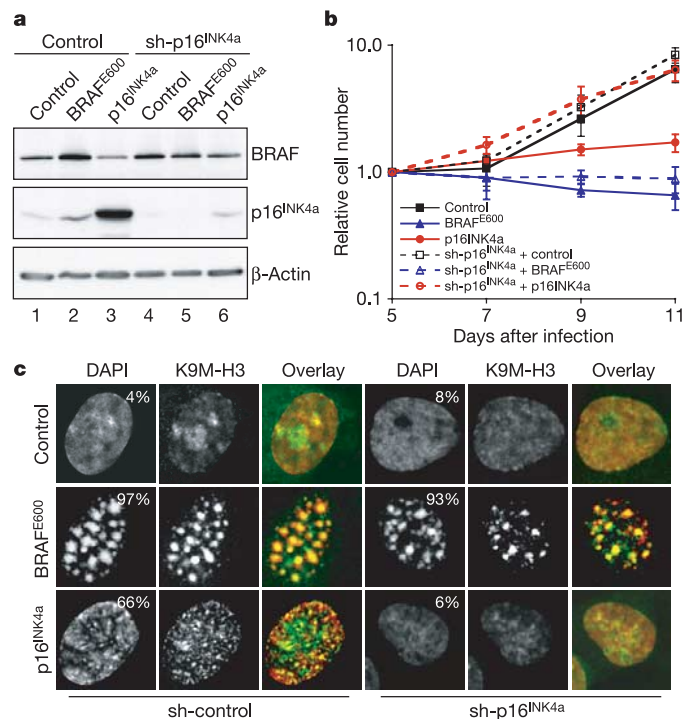


**Figure 2 | Physiological levels of BRAF<sup>E600</sup> induce senescence-like arrest in normal human fibroblasts in a p16<sup>INK4a</sup>-independent manner.** **a–c**, Human BJ<sub>hTERT</sub> cells stably expressing either control or p16<sup>INK4a</sup> shRNA were transduced with a mixture of a retrovirus encoding BRAF<sup>E600</sup> expression and puromycin resistance cassettes, and a retrovirus encoding cassettes for a shRNA targeting both endogenous wild type and ectopic BRAF<sup>E600</sup> and blasticidin resistance (labelled BRAF<sup>E600</sup>). Pharmacological selection for both resistance markers was used to create cells that had stably integrated both the BRAF<sup>E600</sup> expression cassette and the shRNA. The latter alone did not affect proliferative potential (data not shown). As a control, cells were transduced with p16<sup>INK4a</sup>-encoding retrovirus. **a**, Analysis by western blotting with β-actin used as a loading control. **b**, Analysis by proliferation curves. Shown are the results of three independent experiments performed in duplicate with standard deviations. **c**, DAPI staining to detect SAHF (percentage of SAHF-positive cells is indicated in insert) and immunofluorescence for K9M-H3. Note that whereas p16<sup>INK4a</sup> shRNA neutralized senescence induced by ectopic expression of p16<sup>INK4a</sup>, it failed to bypass BRAF<sup>E600</sup>-induced senescence. Even undetectable levels of BRAF<sup>E600</sup> (**a**, compare lanes 4 and 5) were sufficient to induce growth arrest and SAHF, in the absence of p16<sup>INK4a</sup>.



(see Supplementary Fig. 4) and abolished the induction of cell cycle arrest by overexpressed p16<sup>INK4a</sup> (Fig. 2b; see also Supplementary Fig. 2b, c). However, low levels of BRAF<sup>E600</sup> inhibited proliferation and induced SAHF even on p16<sup>INK4a</sup> depletion (Fig. 2b, c; see also Supplementary Fig. 2b, c). Identical observations were made for a p16<sup>INK4a</sup> binding-deficient cyclin-dependent kinase 4 mutant (CDK4<sup>R24C</sup>; see Supplementary Fig. 2e), for a different fibroblast strain (TIG3; see Supplementary Fig. 2f–h) and for fibroblasts explanted from a homozygous p16<sup>INK4a</sup>-deficient ‘Leiden’ patient<sup>20</sup> (see Supplementary Fig. 2i–l). These results suggest that, at least in cultured human fibroblasts, p16<sup>INK4a</sup> is upregulated in response to physiological levels of BRAF<sup>E600</sup>, but is not strictly required for the induction of cell cycle arrest.

Next, we wished to validate *in vivo* our observation that BRAF<sup>E600</sup> induces senescence-like arrest *in vitro*. Given the high frequency of BRAF mutations in both naevi and melanomas<sup>7,12</sup>, we looked for hallmarks of senescence in a panel of resection specimens of human naevi. We first confirmed the presence of the BRAF<sup>E600</sup> mutation in eight specimens of our panel of 23 naevi (see Supplementary Fig. 5). We then used paraffin-embedded as well as cryosections of normal human skin and resection specimens of naevi for further analysis. Virtually all melanocytes within these naevi were growth-arrested, as judged by negative immunohistochemical staining for the proliferation marker Ki-67 (Fig. 3a), in agreement with the literature<sup>8,9</sup>. This was in contrast to epidermal keratinocytes in the same specimens, many of which showed proliferative activity.

As expression of BRAF<sup>E600</sup> in cultured human melanocytes led to cell cycle arrest along with induction of SA-β-Gal activity, we subjected our naevi panel to analysis for this senescence marker.

SA-β-Gal activity has previously been shown to increase in human epidermis as a function of age<sup>15</sup>. To avoid detection of age-induced SA-β-Gal activity, we analysed a panel of congenital naevi obtained from patients under one year of age. Indeed, all 23 naevi analysed displayed high levels of SA-β-Gal activity (Fig. 3a–c). This activity was absent from normal skin melanocytes within the same samples (Fig. 3b, c) and in control samples taken from normal skin (Fig. 3a). In agreement with previous data<sup>21</sup>, SA-β-Gal activity was also absent from freshly isolated, cultured primary human melanocytes (Fig. 1c). Terminally differentiated keratinocytes within the epidermis of the same samples also did not show SA-β-Gal activity (Fig. 3b, c, arrowheads), consistent with previous observations made in young (<39 yr of age) donors<sup>15</sup>. SA-β-Gal activity was similarly lacking from the cells of skin adnexa, such as the sweat gland (Fig. 3b, c, labelled S), and from the dermal mesenchymal cells between the naevus cell nests. Thus, human naevi, largely growth-arrested neoplastic lesions, are positive for the senescence marker SA-β-Gal.

Studies in mouse models and humans indicate that (epi)genetic inactivation of the p16<sup>INK4a</sup> gene is associated with melanomagenesis<sup>9,16,22,23</sup>. Normal melanocytes, scattered alongside the dermal–epidermal junction and surrounded by keratinocytes, had undetectable levels of p16<sup>INK4a</sup> (Fig. 3a). In contrast, naevi invariably contained p16<sup>INK4a</sup>-expressing cells, in agreement with previous observations<sup>9,22</sup>. Of note, we failed to detect any significant upregulation of p53 and p21<sup>CIP1</sup> in naevi (data not shown). Irrespective of the mutational status of BRAF in the naevi, the percentage of p16<sup>INK4a</sup>-positive cells and the intensity of staining per cell was heterogeneous, with a striking mosaic pattern of p16<sup>INK4a</sup> immunopositivity seen in most naevi (Fig. 3a; see also Supplementary Fig. 6; data not shown).

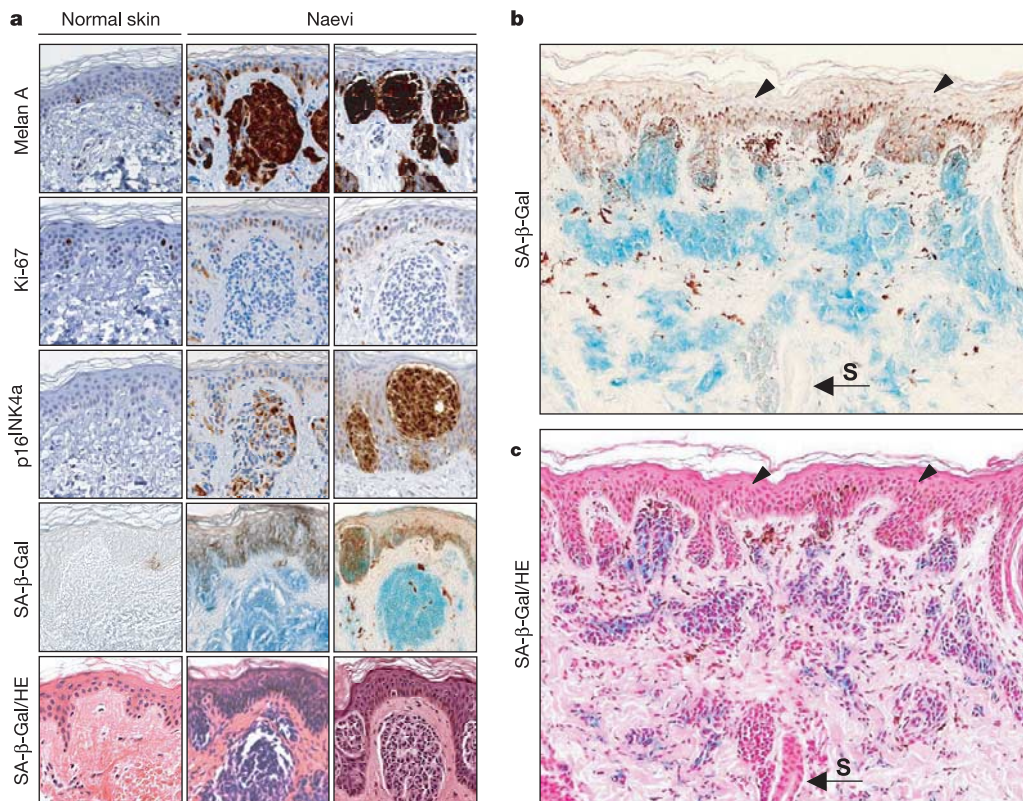


**Figure 3 | Human melanocytic naevi display the hallmarks of senescent cells.** Paraffin-embedded sections of human naevi and normal skin were subjected to immunohistochemistry with the indicated antibodies. **a**, Melan A (brown) identifies melanocytes, MIB1 (brown) recognizes the proliferation marker Ki-67 and p16<sup>INK4a</sup> antibody (brown) detects p16<sup>INK4a</sup>. **a–c**, Frozen sections of human naevi were subjected to SA-β-Gal staining. The blue staining corresponds exactly to the sites of naevus cell nests. All

cells of the epidermis (mostly keratinocytes, arrowheads) and sweat gland (S), as well as dermal cells between the naevus cell nests, are completely negative for SA-β-Gal (**b** and **c**). Note that the brown staining in these samples comes from pigment released by the naevus cells. Where indicated, haematoxylin and eosin (HE) was used as a counter stain on the consecutive (SA-β-Gal-stained) section to visualize the melanocyte lesions, within the context of the surrounding tissue.

Importantly, all melanocytes within these  $p16^{INK4a}$ -mosaic naevi (whether positive or negative for  $p16^{INK4a}$ ) were growth arrested (Fig. 3a; see also Supplementary Fig. 6). Indeed, the lack of proliferation of the naevus melanocytes was associated with positive SA- $\beta$ -Gal staining rather than with  $p16^{INK4a}$  immunoreactivity, thereby closely mimicking BRAF<sup>E600</sup>-expressing melanocytes *in vitro*. As naevi are thought to be clonal<sup>11</sup>, it is unlikely that a differential BRAF mutation pattern underlies the  $p16^{INK4a}$  mosaicism. The observed  $p16^{INK4a}$  mosaicism is in accordance with the occurrence of growth arrest in naevi of homozygous  $p16^{INK4a}$ -deficient Leiden patients<sup>20</sup>. However, the naevi of these patients are increased in number and size compared to those of  $p16^{INK4a}$ -proficient individuals. Together with the mosaic  $p16^{INK4a}$  pattern seen in BRAF<sup>E600</sup>-expressing, growth-arrested melanocytes *in vitro*, these observations suggest that  $p16^{INK4a}$  collaborates with other, yet-to-be-identified factors in the establishment of long-term growth arrest of naevi. Whether  $p16^{INK4a}$  contributes to an irreversible arrest that, once established, no longer requires  $p16^{INK4a}$  (as has been suggested previously<sup>19,24</sup>), or is involved in aspects of melanoma progression other than oncogene-induced senescence remains to be determined. Together these results show that human naevi and BRAF<sup>E600</sup>-expressing melanocytes share three senescence-associated markers: stable growth arrest, heterogeneous induction of  $p16^{INK4a}$  and SA- $\beta$ -Gal activity.

Although these features support oncogene-induced senescence as

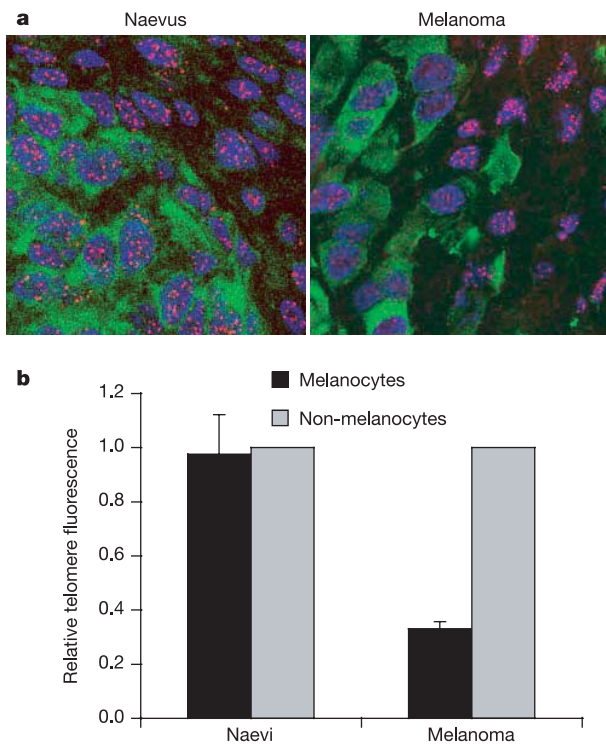


**Figure 4 | No apparent telomere loss in naevi.** **a**, Frozen sections of human naevi and melanomas were subjected to telomere FISH (red). A representative sample is shown; six naevi were analysed (five of which harboured the BRAF<sup>E600</sup> mutation). For reference, sections were also stained with the Melan A antibody (detecting melanocytes in naevus and melanoma, green) and DAPI (blue). Note that in the naevus specimen, both the naevus cells (Melan-A positive) and the stromal compartment (Melan-A negative) are FISH positive. In contrast, melanoma tumour cells, which conceivably have undergone telomere attrition, have a much weaker telomere fluorescence signal than their surrounding stromal cells. The channel overlay is shown (individual channels are shown in Supplementary Fig. 7). **b**, Quantification of the data in **a**, plotted as relative telomere fluorescence in six naevi and three melanomas (both indicated as melanocytes) compared to their respective stromal cells (non-melanocytes) with standard deviations.

the cause for cell cycle arrest of melanocytic naevi, in principle these senescence markers may have been triggered by telomere attrition, which might have resulted from the initial expansion of melanocytes. Indeed, telomere attrition has been previously proposed as a major factor involved in the cell-cycle arrest of naevi<sup>25</sup>. This would be consistent with the clinical observation that congenital naevi (that is, arising before birth) can cover large areas of the body surface, in contrast to naevi acquired later in life, which are usually much smaller. To test this possibility, we performed telomere FISH (fluorescent *in situ* hybridization) on congenital naevus resections. As expected, melanoma metastases, stained as controls, displayed much less fluorescence than their surrounding stromal cells, indicating that this method is sufficiently sensitive to detect differences in telomere length *in situ* (Fig. 4a, b; see also Supplementary Fig. 7). In contrast, we did not observe any significant difference in telomere fluorescence when comparing congenital naevi to surrounding tissues, in agreement with previous observations made in acquired and Spitz naevi<sup>26</sup>. Although we cannot formally rule out the possibility that a single eroded telomere may have triggered the senescence response, one would not expect the other telomeres to remain apparently full length. These results argue in favour of an active oncogene-driven senescence process, rather than senescence triggered by exhaustion of replicative potential resulting from gross telomere attrition.

Our observation that BRAF<sup>E600</sup> initially stimulates moderate melanocyte proliferation supports the hypothesis that it contributes to the initiating events of melanomagenesis. However, our results suggest that, both *in vitro* and *in vivo*, oncogenic BRAF signalling subsequently leads to a growth-inhibitory response, which is associated with the known classical hallmarks of senescence (that is, stable proliferative arrest, an increase in  $p16^{INK4a}$  and the induction of SA- $\beta$ -Gal activity). Our results therefore provide support for a speculative model previously proposed<sup>9,27</sup>, in which BRAF<sup>E600</sup> cannot fully transform human melanocytes, but requires additional, cooperating events for tumour development. Supporting this view, zebrafish expressing a BRAF<sup>E600</sup> transgene develop 'fish-naevi', which require a p53-deficient background to progress to invasive melanomas<sup>28</sup>. Our observations provide evidence of oncogene-induced senescence as a physiological mechanism in humans limiting the progression of premalignant lesions.

## METHODS

**Plasmids.** Gene transfer in normal human melanocytes was achieved with two independent lentiviral vectors (FG12-HA-BRAF<sup>E600</sup>-eGFP and HIV-CS-CG-BRAF<sup>E600</sup>-puro), with comparable phenotypes. pBabe-puro-BRAF<sup>E600</sup> was used to transduce fibroblasts.

The  $p16^{INK4a}$  shRNA sequence corresponds to nucleotides 21–41 (GenBank accession number NM\_000077). The BRAF shRNA sequence was previously described<sup>29</sup>.

**Cell culture, retroviral transduction, cell cycle analysis and proliferation curves.** Normal human melanocytes were isolated from the epidermis of neonatal foreskins. Briefly, foreskins were incubated overnight in trypsinization solution (22.5 mM HEPES, 7.5 mM glucose, 2.25 mM KCl, 100 mM NaCl, 0.75 mM Na<sub>2</sub>HPO<sub>4</sub> and 0.17% trypsin). Dermis and epidermis were separated by scraping. The epidermal compartment was incubated for 3–4 d in 254CF medium (Cascade Biologicals) supplemented with 0.1 mM CaCl<sub>2</sub>, 2% fetal bovine serum and keratinocyte growth supplement (Cascade Biologicals). Melanocytes were subsequently separated from keratinocytes by differential trypsinization. Purity of the melanocytic preparations was estimated by standard immunostaining for HMB-45. For long-term cultures, melanocytes were propagated in 254CF medium in the presence of 0.2 mM CaCl<sub>2</sub> and melanocyte growth supplement (Cascade Biologicals).

BJ cells expressing hTERT (in pBabeHygro) were grown in DMEM/medium 199 (Gibco) in a 4:1 ratio supplemented with 15% fetal bovine serum (PAA Laboratories), 0.1 mM MEM non-essential amino acids (Gibco), 2 mM glutamine (Gibco), 100 units ml<sup>-1</sup> penicillin and 0.1 mg ml<sup>-1</sup> streptomycin.

Lentiviral infections were performed using HEK293T cells as producers of viral supernatants. The Phoenix packaging cell line was used for the generation of ecotropic retroviruses, as described<sup>30</sup>. Amphotropic retroviruses encoding the



ecotropic receptor were generated in HEK293T cells. All infections were carried out as described<sup>30</sup>.

BrdU labelling was carried out for 3 h in reduced growth factor conditions. Proliferation curves were performed as described<sup>6,30</sup>.

**Human tissue samples.** Surgical resection specimens of congenital naevi were obtained from patients in their first year of life. Specimens were fresh frozen and stored for a period of 2 months to 2 years at  $-70^{\circ}\text{C}$  before use.

**Analysis of SA- $\beta$ -galactosidase activity.** Tissues were fixed in 4% formaldehyde for 2 h, washed with 0.2% NP-40, 0.1% Na-deoxycholate, 2 mM  $\text{MgCl}_2$ , 100 mM  $\text{Na}_2\text{HPO}_4$ , pH 6.0 and stained as described<sup>15</sup>. Tissues were post-fixed overnight in 4% formaldehyde and embedded in paraffin. Cultured cells were stained as described<sup>15</sup>.

**Immunohistochemistry and antibodies.** Tissues were fixed in 4% formaldehyde overnight and embedded in paraffin. Paraffin sections were deparaffinized, rehydrated, incubated in 0.1 mM sodium citrate pH 6.0, washed and incubated with peroxidase blocking reagent (S2001; DAKO). The tissue was incubated with the primary antibodies Ab-3 for Melan A (Molecular Probes), MIB-1 for Ki-67 (DAKO) and Ab-4 (16P04) for p16<sup>INK4a</sup> (Molecular Probes). Secondary antibody used was PowerVision + (DPVB + 999HRP; ImmunoLogic). Peroxidase activity was detected with Liquid DAB (K3468; DAKO).

The antibodies used for western blotting were F-7 for BRAF (sc-5284; Santa Cruz), JC8 (MS-889; NeoMarkers) for p16<sup>INK4a</sup>, C-22 for CDK4 (sc-260; Santa Cruz) and AC-74 for  $\beta$ -actin (A5316; Sigma). The antibodies used for immunofluorescence were anti-trimethyl-histone H3 (Lys 9) (07-442; Upstate) and 554070 (BD Pharmingen) for p16<sup>INK4a</sup>. DAPI staining was used to visualize nuclei.

**Telomere FISH.** Tissue sections were prepared for FISH analysis with the 2'-deoxyoligonucleotide N3'  $\rightarrow$  P5' phosphoramidate probe: 5'-(CCCTAA)<sub>3</sub>-TAMRA-3', specific for telomeric sequences. The Melan A antibody Ab-3 was used and also the DNA staining dye DAPI. Images of fluorescein (FITC), TAMRA and DAPI fluorescence were acquired on a digital image microscopy system. The relative telomere length is proportional to the number of hybridized probes. For quantification, the fluorescence signal was determined (using ImageJ software) for all individual telomeres within 12 nuclei per specimen, both for melanocytes (within naevi and melanomas) and for cells within the stromal compartments of both types of lesion, for six independent naevi and three independent melanomas. All measurements have been corrected for background nuclear fluorescence.

Received 19 January; accepted 8 June 2005.

- Hayflick, L. The limited *in vitro* lifetime of human diploid cell strains. *Exp. Cell Res.* **37**, 614–636 (1965).
- Mathon, N. F. & Lloyd, A. C. Cell senescence and cancer. *Nature Rev. Cancer* **1**, 203–213 (2001).
- Lowe, S. W., Cepero, E. & Evan, G. Intrinsic tumour suppression. *Nature* **432**, 307–315 (2004).
- Campisi, J. Senescent cells, tumour suppression, and organismal aging: good citizens, bad neighbors. *Cell* **120**, 513–522 (2005).
- Shay, J. W. & Roninson, I. B. Hallmarks of senescence in carcinogenesis and cancer therapy. *Oncogene* **23**, 2919–2933 (2004).
- Serrano, M., Lin, A. W., McCurrach, M. E., Beach, D. & Lowe, S. W. Oncogenic ras provokes premature cell senescence associated with accumulation of p53 and p16<sup>INK4a</sup>. *Cell* **88**, 593–602 (1997).
- Pollock, P. M. *et al.* High frequency of BRAF mutations in nevi. *Nature Genet.* **33**, 19–20 (2003).
- Kuwata, T., Kitagawa, M. & Kasuga, T. Proliferative activity of primary cutaneous melanocytic tumours. *Virchows Arch. A Pathol. Anat. Histopathol.* **423**, 359–364 (1993).
- Bennett, D. C. Human melanocyte senescence and melanoma susceptibility genes. *Oncogene* **22**, 3063–3069 (2003).
- Chin, L., Merlino, G. & DePinho, R. A. Malignant melanoma: modern black plague and genetic black box. *Genes Dev.* **12**, 3467–3481 (1998).
- Robinson, W. A. *et al.* Human acquired naevi are clonal. *Melanoma Res.* **8**, 499–503 (1998).
- Davies, H. *et al.* Mutations of the BRAF gene in human cancer. *Nature* **417**, 949–954.
- Wellbrock, C. *et al.* V599E-BRAF is an oncogene in melanocytes. *Cancer Res.* **64**, 2338–2342 (2004).
- Mooi, W. J. & Krausz, T. *Biopsy Pathology of Melanocytic Disorders* 56–105 (Chapman & Hall Medical, London, 1992).
- Dimri, G. P. *et al.* A biomarker that identifies senescent human cells in culture and in aging skin *in vivo*. *Proc. Natl Acad. Sci. USA* **92**, 9363–9367 (1995).
- Sharpless, E. & Chin, L. The INK4a/ARF locus and melanoma. *Oncogene* **22**, 3092–3098 (2003).
- Zhu, J., Woods, D., McMahon, M. & Bishop, J. M. Senescence of human fibroblasts induced by oncogenic Raf. *Genes Dev.* **12**, 2997–3007 (1998).
- Lin, A. W. *et al.* Premature senescence involving p53 and p16 is activated in response to constitutive MEK/MAPK mitogenic signalling. *Genes Dev.* **12**, 3008–3019 (1998).
- Narita, M. *et al.* Rb-mediated heterochromatin formation and silencing of E2F target genes during cellular senescence. *Cell* **113**, 703–716 (2003).
- Gruis, N. A. *et al.* Homozygotes for CDKN2 (p16) germline mutation in Dutch familial melanoma kindreds. *Nature Genet.* **10**, 351–353 (1995).
- Bandyopadhyay, D. *et al.* The human melanocyte: a model system to study the complexity of cellular aging and transformation in non-fibroblastic cells. *Exp. Gerontol.* **36**, 1265–1275 (2001).
- Wang, Y. L., Uhara, H., Yamazaki, Y., Nikaido, T. & Saida, T. Immunohistochemical detection of CDK4 and p16<sup>INK4</sup> proteins in cutaneous malignant melanoma. *Br. J. Dermatol.* **134**, 269–275 (1996).
- Kamb, A. *et al.* A cell cycle regulator potentially involved in genesis of many tumour types. *Science* **264**, 436–440 (1994).
- Beausejour, C. M. *et al.* Reversal of human cellular senescence: roles of the p53 and p16 pathways. *EMBO J.* **22**, 4212–4222 (2003).
- Bastian, B. C. Understanding the progression of melanocytic neoplasia using genomic analysis: from fields to cancer. *Oncogene* **22**, 3081–3086 (2003).
- Miracco, C. *et al.* Quantitative *in situ* evaluation of telomeres in fluorescence *in situ* hybridization-processed sections of cutaneous melanocytic lesions and correlation with telomerase activity. *Br. J. Dermatol.* **146**, 399–408 (2002).
- Peeper, D. S. & Mooi, W. J. Pathogenesis of melanocytic naevi: growth arrest linked with cellular senescence? *Histopathology* **41**, S139–S143 (2002).
- Patton, E. E. *et al.* BRAF mutations are sufficient to promote nevi formation and cooperate with p53 in the genesis of melanoma. *Curr. Biol.* **15**, 249–254 (2005).
- Hingorani, S. R., Jacobetz, M. A., Robertson, G. P., Herlyn, M. & Tuveson, D. A. Suppression of BRAF(V599E) in human melanoma abrogates transformation. *Cancer Res.* **63**, 5198–5202 (2003).
- Peeper, D. S. *et al.* A functional screen identifies hDRIL1 as an oncogene that rescues RAS-induced senescence. *Nature Cell Biol.* **4**, 148–153 (2002).

**Supplementary Information** is linked to the online version of the paper at [www.nature.com/nature](http://www.nature.com/nature).

**Acknowledgements** We thank D. Atsma, E. Mesman and J. Zevenhoven for help with immunohistochemistry; S. Douma for analytical support; L. Oomen, L. Brocks and J. van Rheenen for help with microscopy; N. Gruis and C. Out for p16<sup>INK4a</sup>-deficient fibroblasts; L. Zaal and A. van der Wal for help with obtaining congenital naevus specimens; M. Voorhoeve and R. Agami for pRetroSuper, pRetroSuper-Blasticidin and pRetroSuper-GFP; S. Gryaznov for the telomere probe; R. Beijersbergen and M. van Lohuizen for reagents; G. Abou-Rjaily for help with lentiviral infections; P. Krimpenfort and colleagues in the Peeper laboratory for discussions; R. Bernards for support; and M. van Lohuizen and A. Berns for suggestions and reading of the manuscript. M.S.S. is supported by an NIH grant. M.S.S. is a V Foundation for Cancer Research Scholar. L.C.W.V., T.K. and D.S.P. were supported by the Netherlands Organization for Scientific Research (NWO).

**Author Information** Reprints and permissions information is available at [npg.nature.com/reprintsandpermissions](http://npg.nature.com/reprintsandpermissions). The authors declare no competing financial interests. Correspondence and requests for materials should be addressed to D.S.P. ([d.peeper@nki.nl](mailto:d.peeper@nki.nl)) or W.J.M. ([wj.mooi@vmuc.nl](mailto:wj.mooi@vmuc.nl)).